J|A|C|S
COMMUNICATIONS

Published on Web 12/12/2002

Charge Ordering in Lithium Vanadium Phosphates: Electrode Materials for Lithium-Ion Batteries

Shih-Chieh Yin,[†] Hiltrud Grondey,[‡] Pierre Strobel,[§] Huan Huang,[†] and Linda F. Nazar*,[†]

Department of Chemistry, University of Waterloo, Waterloo, Ontario, Canada N2L 3G1, Department of Chemistry, University of Toronto, Toronto, Ontario, Canada, and Laboratoire de Crystallographie, CNRS, Grenoble, France

Received October 16, 2002; E-mail: lfnazar@uwaterloo.ca

Rechargeable lithium-ion cells are considered to be the most advanced energy storage systems. Commercial cells utilize cobalt-based oxides as the positive electrode,[1] but its high cost and toxicity prohibit use in large-scale applications. In an intensive search for alternative materials, phosphates such as $LiFePO_4$ have emerged as among the most promising.[2−6] In addition to possessing high redox potentials and good Li^+ transport, phosphates exhibit remarkable electrochemical and thermal stability.[7,8] Monoclinic $Li_3V_2(PO_4)_3$ displays the highest capacity, where full reversible extraction has been achieved at fast rates.[9,10] Yet electron/Li^+ location and transport within this lattice, as well as structural transitions related to lithium content, are poorly understood so far. The understanding of such phenomena is critical to the search for new materials as well as improvements in the current ones and forms the subject of this work. $Li_3V_2(PO_4)_3$ contains both mobile Li cations and redox-active metal sites housed within a rigid phosphate framework. The thermodynamically more stable monoclinic (M) form,[10,11] unlike the rhombohedral phase,[12] exhibits a complex series of two-phase transitions on Li extraction, followed by a solid solution regime on lithium reinsertion. Here, using a combination of neutron diffraction[13] and ^{7}Li solid-state NMR,[14] we reveal that vanadium charge ordering and lithium site ordering drive the phase transitions. Most important, for the first time, we show that electron transport is pinned even on short time scales.

The electrochemical voltage-composition curve obtained by a current-pulse technique for lithium extraction/reinsertion in M−$Li_3V_2(PO_4)_3$ is shown in Figure 1. The plateaus in the oxidation curve correspond to the transitions between the single phases $Li_xV_2(PO_4)_3$: $x = 2.5$, 2.0, 1.0, and 0. The existence of these compositions has also been predicted by first principle calculations.[15] Although solid solution behavior is exhibited on reduction at both fast and quasi-equilibrium rates, the oxidation process is reversible on the second cycle even during fast-rate cycling.[10] To understand the nature of the transitions, the $x = 2.0$, 1.0, and 0.0 compositions were prepared by stoichiometric chemical oxidation of $Li_3V_2(PO_4)_3$ with 1 M NO_2BF_4 in acetonitrile, to provide large quantities of materials free of binder and electrolyte. The PND patterns for $x = 2.0$ and 1.0 were fit using least-squares (Rietveld) methods.[16] Both refinements converged with excellent statistics and small residuals, as summarized in Table 1. The resultant structures are depicted in Figure 2, along with an expanded view of the lithium coordination environments.

The unit cell of the starting phase $Li_3V_2(PO_4)_3$ (Figure 2a-i)[10] contains two VO_6 octahedra that are distinct, but almost the same within the limits of crystallographic statistics (average V−O distances V(1) 2.003 and V(2) 2.006 Å), and three Li ions. The latter reside in one tetrahedral site (Li_1) and two pseudotetrahedral

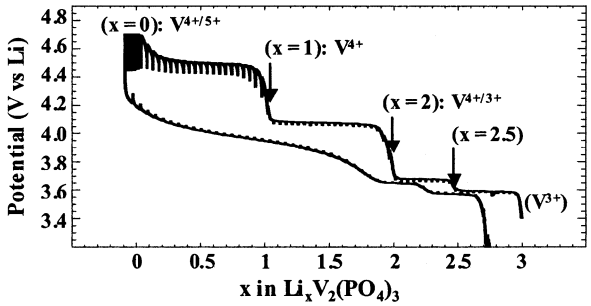

Figure 1. Galvanostatic intermittent titration plot for Li extraction from $Li_3V_2(PO4)_3$ showing the single phase compositions $LixV_2(PO_4)_3$ ($x = 3.0 \rightarrow 0.0$), followed by Li insertion. Regions characterized by a short relaxation spike indicate fast equilibration. The current was curtailed at each step corresponding to an equivalent rate of *C*/500.

Table 1. Rietveld Refinements for $Li_xV_2(PO_4)_3$ in $P2_1/n$

	a (Å)	*b* (Å)	*c* (Å)	β (deg)	χ^2	R_{wp}
$x = 2$	8.4567	8.6208	11.8958	90.236	4.80	4.83%
$x = 1$	8.3006	8.5176	11.6526	89.605	2.93	3.86%

sites (Li_2 and Li_3), which possess an additional long Li−O bond (Figure 2a-iii). These sites are readily resolved in the ^{7}Li NMR spectrum at 103, 52, and 17 ppm (Figure 2a-ii). The shift of the three ^{7}Li NMR lines to high frequency arises from the well-known Fermi contact shift.[17] Transfer of electron density from the V^{3+} t_{2g}-like orbitals to the Li 2s orbital gives rise to a positive shift, as shown for other materials.[18,19] By comparison, the rhombohedral phase of $Li_3V_2(PO_4)_3$) with a unique Li site displays a single line at an intermediate value of 85 ppm.[14] The magnitude of the Fermi contact shift is dependent not only on the number of d-electrons (all d^2 here) but also on Li−O-M bond lengths and bond angles.[20]

The structure of the phase obtained after extracting one Li, $Li_2V_2(PO_4)_3$, is shown in Figure 2b-i. The lattice maintains $P2_1/n$ symmetry and a very similar framework. We see that Li_3, the highest energy site based on bond-sum calculations,[21] is extracted, while Li_2 shifts to a tetrahedral site very similar to that of Li_1 (Figure 2b-iii), with the same geometry and average Li−O bond length.[22] Most important, clear evidence for V^{3+}/V^{4+} ordering is demonstrated by both the structural and the NMR data. The average V(1) bond length is contracted by 0.1 Å to 1.908 Å, whereas V(2)−O (1.989 Å) remains almost the same as that in the original V^{3+} structure. This gives rise to charge ordering of the V^{n+} to form "columns" of V^{3+} or V^{4+} along the *a*-axis and *b*-axis. The charge ordering is also unequivocally demonstrated by NMR. Despite the almost identical geometry of the two sites, *two* isotropic lines are observed at 77 and 143 ppm. Their shift difference is due to the one electron difference in orbital transfer between $Li_1-O-V(1)d^1$ and $Li_2-O-V(2)d^2$, that is, the magnitude of the hyperfine interaction between the two sites. The contribution of the t_{2g}

† University of Waterloo.
‡ University of Toronto.
§ CNRS.
* Author to whom correspondence is addressed: lfnazar@uwaterloo.ca.

10.1021/ja028973h CCC: $25.00 © 2003 American Chemical Society

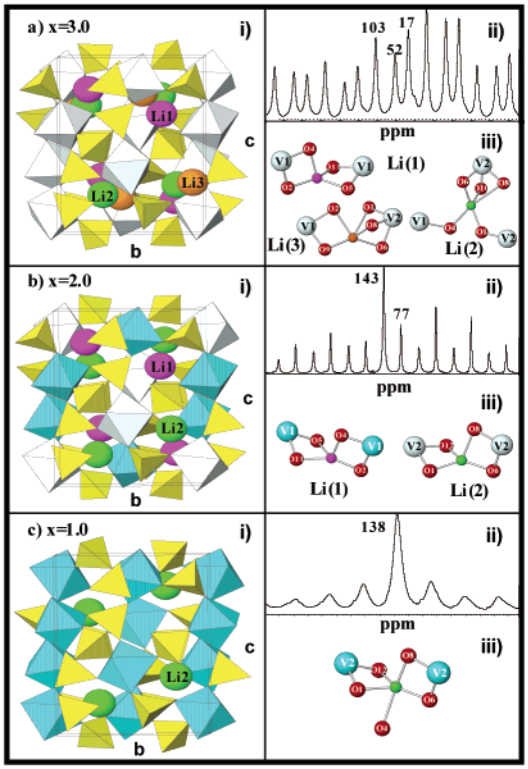

Figure 2. Description of all phases where i − structure, ii − NMR, and iii − coordination environment of Li: (a) $x = 3.0$; (b) $x = 2.0$; (c) $x = 1.0$. Average bond lengths in $Li_2V_2(PO_4)_3$: Li_1−O, 1.972 Å; Li_2−O, 1.973 Å; in $LiV_2(PO_4)_3$: Li_2−O, 1.98 Å with one additional bond to O_4 at 2.45 Å. Isotropic peaks are marked in the spectra; the remainder are spinning sidebands.

electron(s) can thus be estimated at about 65−77 ppm, in good accord with the value determined from studies of $LiMPO_4$ of 70 ppm.[19] That the effects here are because of the hyperfine interaction is confirmed by temperature-dependent NMR measurements.

These results show the two-phase transition at 3.65 V; electrons are extracted from the V(1) sites. They remain pinned on the V(2) sites on both NMR (long) and diffraction (short) time scales. Subsequent Li/electron extraction gives $Li_{1.0}V_2(PO_4)_3$, whose structure is shown in Figure 2c-i. Li_1 is preferentially extracted due to the repulsion energy of the Li_1^+−$V(1)^{4+}$ pair in $Li_2V_2(PO_4)_3$, which destabilizes this site. The monoclinic symmetry of the lattice is preserved, although a significant twist in the structure results in a five-coordinate Li_2 environment (Figure 2c-iii). The structure refinement again confirms redox chemistry, as V(2)−O distances decrease to a value (1.907 Å) similar to that in V(1)−O (1.908 Å), in agreement with the unique V^{4+} oxidation state. In accord, the ^{7}Li NMR spectrum shows a single site displaying a resonance at 138 ppm (Figure 2c-ii). DFT calculations are underway to quantify the exact origins of the changes in the NMR shifts.

Extraction of the third Li ion/electron (upper plateau at 4.55 V) to form $V_2(PO_4)_3$ results in a mixed V^{4+}/V^{5+} state which our studies indicate does *not* display valence ordering. The monoclinic structure (based on both XRD[10] and PND) is similar to the others described here and will be reported in a subsequent paper along with the other single and solid solution phases.

Although evidence for electron ordering has been previously sought in several electrochemically active phosphates,[23] this is the first time it has been observed. The existence of ordered valence states in $Li_2V_2(PO_4)_3$ demonstrates the electrons are pinned even on a long time scale; by extension, this may also apply to the other single phase compositions. Each plateau in the V versus x curve corresponds to a two-phase transition involving the reorganization of electrons and Li ions within the lattice. The energies of structures spanning the phase transition are governed by the site potential of the Li^+ ion and their interaction with the V^{n+} ions in the lattice. The question remains as to whether the Li-site ordering drives the electron ordering or the converse. Most likely, as our results suggest, the two are inextricably coupled, resulting in paired electron/ion transport. These findings explain the complex steps displayed in the voltage-composition curve of $Li_{3-x}V_2(PO_4)_3$, but they are directly relevant to other materials. Our results also bear on the principle of using valence substitution to drive the formation of solid solution regimes, important to the practical implementation of these phosphates as electrode materials. Even more intriguing are phase transitions that span lithium compositions with similar structures, as in $LiFePO_4$.

Acknowledgment. We thank the Institut Laue-Langevin and E. Suard (ILL) for her able assistance. We are grateful to W. P. Power (Waterloo) and M. Anne (CNRS, Grenoble) for helpful discussions. L.F.N. acknowledges NSERC for funding.

References

(1) Thackeray, M. M.; Thomas, J. O.; Whittingham, M. S. *MRS Bull.* **2000**, *25(3)*, 39.
(2) Padhi, A. K.; Nanjndaswamy, K. S.; Goodenough, J. B. *J. Electrochem. Soc.* **1997**, *144*, 1188.
(3) Ravet, N.; Goodenough, J. B.; Besner, S.; Simoneau, M.; Hovington, P.; Armand, M. *Abstract #127*, 196th ECS Meeting, Honolulu, HI; The Electrochemical Society: Pennington, NJ, 1999.
(4) Andersson, A. S.; Thomas, J. O.; Kalska, B.; Häggström, L. *Electrochem. Solid-State Lett.* **2000**, *3*, 66.
(5) Yamada, A.; Hinokuma, K. *J. Electrochem. Soc.* **2001**, *148*, A224.
(6) Huang, H.; Yin, S.-C.; Nazar, L. F. *Electrochem. Solid-State Lett.* **2001**, *4*, A170.
(7) Padhi, A. K.; Manivannan, K. S. V.; Goodenough, J. B. *J. Electrochem. Soc.* **1998**, *145*, 1518.
(8) Nanjundaswamy, K. S.; Padhi, A. K.; Goodenough, J. B.; Okada, S.; Ohtsuka, H.; Arai, H.; Yamaki, J. *Solid State Ionics* **1996**, *92*, 1.
(9) Saïdi, M. Y.; Barker, J.; Huang, H.; Adamson, G. *Electrochem. Solid-State Lett.* **2002**, *5*, A149.; U.S. Patent 5871866, 1999.
(10) Huang, H.; Yin, S.-C.; Kerr, T.; Nazar, L. F. *Adv. Mater.* **2002**, *14*, 1525.
(11) Ohkawa, H.; Yoshida, K.; Saito, M.; Uematsu, K.; Toda, K.; Sato, M. *Chem. Lett.* **1999**, 1017.
(12) Gaubicher, J.; Goward, G.; Wurm, C.; Masquelier, C.; Nazar, L. F. *Chem. Mater.* **2000**, *12*, 3240.
(13) About 2 g of each sample was loaded in a hermetically sealed vanadium can in an Ar filled glovebox. Neutron diffraction experiments were carried out on the high-resolution diffractometer D2B at the Institut Laue-Langevin, France, at a wavelength, $\lambda = 1.5940$ Å. Data were collected over the range $2\theta = 10-160°$, using a step size of 0.05°.
(14) Samples were hermetically sealed in a zirconia rotor fitted with airtight Kel-F caps in an Ar-filled glovebox. The spectra were recorded on a Bruker DSX200 at the resonance frequency of ^{7}Li (77.789 MHz). A single pulse sequence was used, with a 2.5 μs (90°) pulse length and a repetition time of 2 s. The spinning speeds were varied from 6 to 11.5 kHz to identify the isotropic chemical shifts.
(15) Morgan, D.; Ceder, G.; Saidi, Y.; Barker, J.; Adamson, G. *Abstract 349*, 11th IMLB, Monterey, CA, June 2002; *J. Power Sources*, in press.
(16) The lattice parameters were first determined by a full-pattern (LeBail) fit that also confirmed the presence of a single phase. Rietveld refinement was performed on a model based on the single-crystal structure of $Li_3V_2(PO_4)_3$. The Li positions were located by Fourier difference mapping, and the refinement was completed with these sites included.
(17) Marichal, C.; Hirschinger, J.; Granger, P.; Menetrier, M.; Rougier, A.; Delmas, C. *Inorg. Chem.* **1995**, *34*, 1773.
(18) Lee, Y. L.; Wang, F.; Grey, C. P. *J. Am. Chem. Soc.* **1998**, *120*, 12601.
(19) Tucker, M. C.; Doeff, M. M.; Richardson, T. J.; Finones, R.; Cairns, E. J.; Reimer, J. A. *J. Am. Chem. Soc.* **2002**, *124*, 3832.
(20) Aatiq, A.; Menetrier, M.; Croguennec, L.; Suard, E.; Delmas, C. *J. Mater. Chem.* **2002**, *12*, online advance article.
(21) Bond sum calculations for Li(1), 1.043; Li(2), 1.018; Li(3), 0.915, see: Brown, I. D. *Chem. Soc. Rev.* **1978**, *7*, 359.
(22) These two are essentially pseudosymmetry sites because the lattice is very close to orthorhombic. Attempts to refine the cell in an orthorhombic space group such as *Pbna* resulted in higher convergence values.
(23) Eyob, P.; Andersson, A. S.; Thomas, J. O. *J. Mater. Chem.* **2002**, *12*, 1.

JA028973H